

## Electrochemical Detection of Bisphenol A Using Graphene-Modified Glassy Carbon Electrode

B. Ntsendwana<sup>1</sup>, B.B. Mamba<sup>1</sup>, S. Sampath<sup>2</sup>, O.A. Arotiba<sup>1,\*</sup>

<sup>1</sup> Department of Chemical Technology, University of Johannesburg, P.O. Box 17011, Doornfontein, 2028, South Africa.

<sup>2</sup> Department of Inorganic and Physical Chemistry, Indian Institute of Science, Bangalore, 560012, India

\*E-mail: [oarotiba@uj.ac.za](mailto:oarotiba@uj.ac.za)

Received: 18 January 2012 / Accepted: 25 February 2012 / Published: 1 April 2012

---

Graphene's nano-dimensional nature and excellent electron transfer properties underlie its electrocatalytic behavior towards certain substances. In this light, we have used graphene in the electrochemical detection of bisphenol A. Graphene sheets were produced via soft chemistry route involving graphite oxidation and chemical reduction. X-ray diffraction, Fourier transform infra-red (FT-IR) and Raman spectroscopy were used for the characterization of the as-synthesized graphene. Graphene exhibited amorphous structure in comparison with pristine graphite from XRD spectra. FT-IR showed that graphene exhibits OH and COOH groups due to incomplete reduction. Raman spectroscopy revealed that multi-layered graphene was produced due to low intensity of the 2D-peak. Glassy carbon electrode was modified with graphene by a simple drop and dry method. Cyclic voltammetry was used to study the electrochemical properties of the prepared graphene-modified glassy carbon electrode using potassium ferricyanide as a redox probe. The prepared graphene-modified glassy carbon electrode exhibited more facile electron kinetics and enhanced current of about 75% when compared to the unmodified glassy carbon electrode. The modified electrode was used for the detection of bisphenol A. Under the optimum conditions, the oxidation peak current of bisphenol A varied linearly with concentration over a wide range of  $5 \times 10^{-8} \text{ mol L}^{-1}$  to  $1 \times 10^{-6} \text{ mol L}^{-1}$  and the detection limit of this method was as low as  $4.689 \times 10^{-8} \text{ M}$ . This method was also employed to determine bisphenol A in a real sample

---

**Keywords:** graphene, bisphenol A, electrochemical detection, glassy carbon electrode, differential pulse voltammetry.

### 1. INTRODUCTION

There is a growing interest in the possible health threat posed by endocrine-disrupting chemicals (EDCs). Bisphenol A (BPA), 2,2-bis(4-hydroxyphenyl) propane is a commonly used raw

material in the production of polycarbonate (PC) and epoxy resin (EP) which are widely used as plastic food containers, food can linings and water bottles [1].

The residual BPA in PC bottles, due to incomplete reaction, may leach into food and subsequently ingest by human. BPA and its derivatives have been widely distributed in the natural environment and surface water during the manufacturing process or the degradation products of plastics. Exposure to BPA has resulted to extensive human health effects since it exhibits estrogenic activity. These include reproduction dysfunctions, endometrial hyperplasia, recurrent miscarriages, abnormal karyotypes and polycystic ovarian syndrome [1,2]. Therefore, it is quite urgent to search for an efficient approach for the degradation and detection of such a chemical so as to minimize its contamination

BPA has been determined with the use of GC/MS or HPLC [3]. These instrumental methods are expensive and need complicated pretreatment and are not applicable to on-site monitoring. Electrochemical techniques have been recognized as suitable methods for detection of phenolic compounds due to their fast response, good reliability, low energy consumption, simple operation, and high sensitivity [1,4,5]. Oxidation of BPA occurs at bare electrodes resulting in the formation of dimmers which poison the electrode thus decreasing the oxidation current. Therefore, in order to enhance sensitivity, electrodes should be modified with materials that exhibit electrocatalytic activity towards the analyte.

Graphene is a zero-band gap semiconductor which consists of two-dimensional sheet of carbon atoms arranged in six-member rings (hexagonal configuration) with atoms connected by  $sp^2$  bonds [6,7]. These bonds and this electron configuration provide the extraordinary properties of graphene, such as a very large surface area ( $2630 \text{ m}^2/\text{g}$ , twice that of single-walled carbon nanotubes) which results in excellent adsorptivity [8,9].

Furthermore, high quality graphene sheets are capable of allowing electrons to travel without scattering mobilities at room temperature thus making them electron sinks or electron transfer bridges [10]. This electronic property makes graphene a suitable material for the enhancement of oxidation current of BPA. This work involves the preparation of graphene- modified glassy carbon electrode and the study of its electrocatalytic activity towards detection of BPA

## 2. MATERIALS AND METHODS

### 2.1 Apparatus and reagents

Natural graphite, bisphenol A (BPA, 97%),  $\text{NaNO}_3$ ,  $\text{H}_2\text{SO}_4$  (98%),  $\text{H}_2\text{O}_2$  (30 %),  $\text{HCl}$  (5%), Dimethylformamide (DMF),  $\text{K}_3\text{Fe}(\text{CN})_6$ ,  $\text{KNO}_3$  were purchased from Sigma Aldrich (South Africa). Hydrazine solution,  $\text{NaH}_2\text{PO}_4 \cdot \text{H}_2\text{O}$  and  $\text{NH}_3$  were purchased from Merck.

FT-IR spectra of the prepared pellets were measured using a Perkin Elmer Spectrum 100 spectrometer with pure KBr as the background. Raman spectra of the pristine graphite, graphene oxide, and graphene powders were measured by using Perkin Elmer Raman Micro 200 system with 785 nm diode laser excitation at room temperature. XRD measurements were performed using a

monochromatic Cu K $\alpha$  radiation of 1.54060 Å, current of 40 mA and energy of 40 kV. All electrochemical experiments were performed with autolab electrochemical analyzer using a three electrode system. A glassy carbon electrode (or graphene modified glassy carbon electrode) serves as the working electrode, a platinum wire as the auxiliary electrode, and an Ag/AgCl (3.0 M KCl) as the reference electrode. Cyclic voltammetry and electrochemical impedance spectroscopy (EIS) were used to study electrochemical properties of graphene-modified GCE. EIS was carried out within the frequency range of 0.1 Hz to 105 Hz and bias potential of 0.189 V. The detection of BPA was carried out using cyclic voltammetry and differential pulse voltammetry (pre-concentration time = 5s, scan rate = 20 mV s<sup>-1</sup> and pulse amplitude = 50 mV).

## 2.2 Synthesis of graphene

Graphene sheets were synthesized from oxidation of graphite using a modified Hummer's method [11]. Approximately 2.5 g of natural graphite powder and 1.25 g NaNO<sub>3</sub> were mixed with 60 mL H<sub>2</sub>SO<sub>4</sub> in 250 mL flask and stirred for 30 min in an ice bath. About 7.5 g KMnO<sub>4</sub> was added slowly to the suspension while maintaining the reaction temperature lower than 20 °C. The reaction mixture was left overnight at room temperature. About 75 mL of deionised water was added and then increased with effervescence NaH<sub>2</sub>PO<sub>4</sub>.H<sub>2</sub>O (effervescences are used to quickly increase temperature) and stirred at 98 °C for a day. After the addition of 25 mL H<sub>2</sub>O<sub>2</sub> (30%), the mixture was then washed with 5% HCl and water and then centrifuged for 20 min at 5000 rpm. After filtration and drying at 40 °C, graphene oxide was obtained as a gray powder. The graphene oxide was then reduced with hydrazine at 90 °C for 20 hrs. The final products were then washed with deionised water and dried at 60 °C.

**Pellet making:** The as-received natural graphite powder and synthesized graphene oxide and graphene sheets were mixed with KBr powder and compressed into a transparent tablet for measurements. The FT-IR spectra of the prepared pellets were measured with pure KBr as the background.

## 2.3 Preparation of graphene -modified glassy carbon electrode

A bare GCE was polished with alumina powder, rinsed ultrasonically with deionized water and dried at room temperature before use. Approximately 1 mg of graphene and graphene oxide were dispersed in 1 mL of DMF and ultrasonicated for 30 min. About 5 μL of the graphene oxide and graphene suspension was cast on the surface of GCE and dried in air. Prior to use, the modified electrode was carefully rinsed with water to remove the loosely attached graphene on the electrode surface.

#### 2.4. Extraction of the Bisphenol A samples

Bisphenol A was extracted from mineral water bottle using the method reported by Kuramitz et al. [12]. Briefly, the mineral water bottle was cut into pieces (2.00 g), and ultrasonicated for 30 min in 30 mL ultra pure water. The product was then immersed in 70 °C oil bath for 48 hrs. After filtration, the liquid phase was collected in 100 mL flask. The extraction process was repeated twice. After that 4.00 mL of each sample was added into 4.00 mL pH 7 phosphate buffer and stored at 4 °C before analysis. The detection of BPA was carried out using cyclic voltammetry and differential pulse voltammetry.

### 3. RESULTS AND DISCUSSION

#### 3.1. Characterization of graphene sheets

**Raman spectroscopy:** Raman spectra of graphite, graphene oxide (GO) and graphene are shown in Figure 1. The spectrum for graphite Figure 1(a) shows typical D- peak at  $1317\text{ cm}^{-1}$  and G- peak at  $1581\text{ cm}^{-1}$ . The G peak corresponds to optical  $E_{2g}$  phonons at the Brillouin zone center and is due to bond stretching of  $sp^2$  carbon pairs in both rings and chains [13]. The D peak is due to the breathing mode of aromatic rings and requires a defect for its activation. D-peak intensity serves as a measure of the degree of disorder. Therefore, from the D-intensity of graphite, it can be said that, graphite exhibits highly ordered structure.

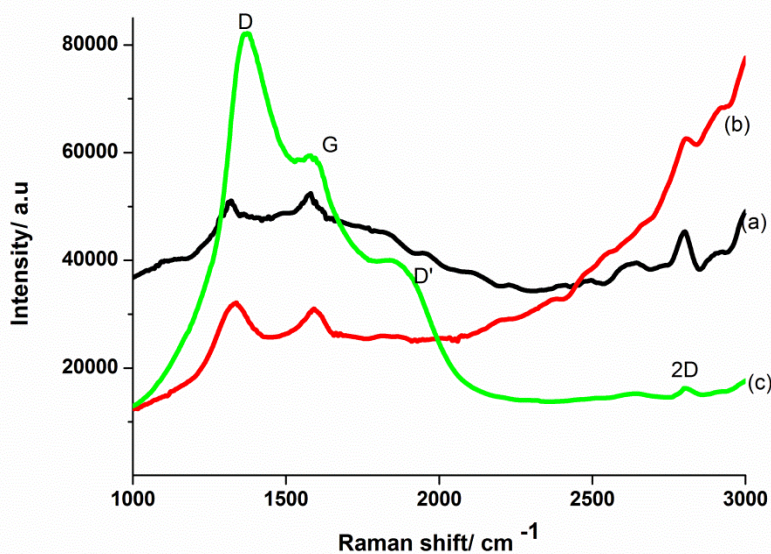


**Figure 1.** Raman shift of (a) graphite powder, (b) graphene oxide and (c) graphene sheets.

Furthermore, the D-peak of GO shown in Figure 1(b), has increased intensity which is attributed to the presence of functional groups. However, the D-intensity of graphene is still high even after reduction as shown in Figure 1 (c). This may be due to the fact that hydrazine is able to reduce the epoxy functional group only. The G- peak of graphene has split into two peaks, G-peak ( $1583\text{ cm}^{-1}$ ) and D'-peak ( $1620\text{ cm}^{-1}$ ). The splitting is due to randomly distributed impurities which can interact with the extended phonon modes of graphene. The 2D- peak (the overtone of the D-peak) at  $2808\text{ cm}^{-1}$  is observed. Its shift and shape has been correlated with the number of graphene layers [14]. This is mainly because in the multi-layer graphene, the shape of 2D band is different from that in the single-layer graphene. The 2D band in the single-layer graphene is much more intense and sharper as compared to the 2D band in multi-layer graphene. Therefore, from the spectrum of graphene it can be concluded that a multi-layer graphene was synthesized.

**FT-IR spectroscopy:** Figure 2 shows FT-IR spectra of graphite, GO and graphene sheet respectively. The graphite spectrum illustrates O-H broad peak at  $3148\text{ cm}^{-1}$  resulting from intercalated water; C=C at  $1630\text{ cm}^{-1}$  which is assigned to the skeletal vibrations of graphitic domains. The spectrum of the GO in Figure 2(b) shows several characteristic peaks corresponding to O-H vibration at  $3148\text{ cm}^{-1}$ , C=O stretching at  $1726\text{ cm}^{-1}$ , C=C skeletal vibration from unoxidized graphitic domains at  $1627\text{ cm}^{-1}$ , O-H deformation at  $1409\text{ cm}^{-1}$ , epoxy symmetrical ring deformation at  $1174\text{ cm}^{-1}$ , C-O stretching mixed with C-OH bending at  $1032\text{ cm}^{-1}$  and O-H-O out of plane wagging at  $829\text{ cm}^{-1}$ . After reduction as seen in Figure 2(c), the peaks corresponding to C=O stretching at  $1726\text{ cm}^{-1}$ , epoxy symmetrical ring deformation at  $1174\text{ cm}^{-1}$  disappeared while the peak at  $1589\text{ cm}^{-1}$  (C=C) was retained. This showed that reduction results in the formation of  $\text{sp}^2$  carbon structure. Thus it can be concluded that graphene sheets were produced via reduction of graphene oxide.

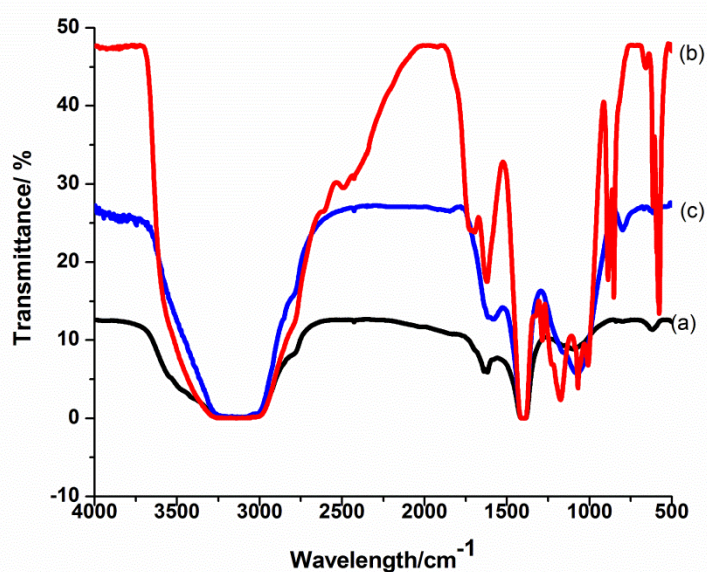


**Figure 2.** FT-IR spectra of (a) graphite powder, (b) graphene oxide (c) graphene sheets.

**X-ray Diffractometry** (spectra not shown): The XRD spectrum of graphite showed its typical peaks at  $26.39\text{\AA}$  and  $54.77\text{\AA}$  which denote the reflections (002) and (004), respectively. The graphite exhibit well defined peaks which confirm its high crystallinity. The XRD pattern of GO in shows characteristic peaks at  $2\theta = 26\text{\AA}$  and  $44\text{\AA}$ . It can be seen that GO is amorphous due to the presence of functional groups in its structure. After reduction to graphene, the peaks were retained but with less amorphous structure.

### 3.2. Electrochemical characterization of graphene-modified GCE.

The electrochemical properties of graphene modified GCE were studied using potassium ferricyanide as a redox marker (Figure 3).

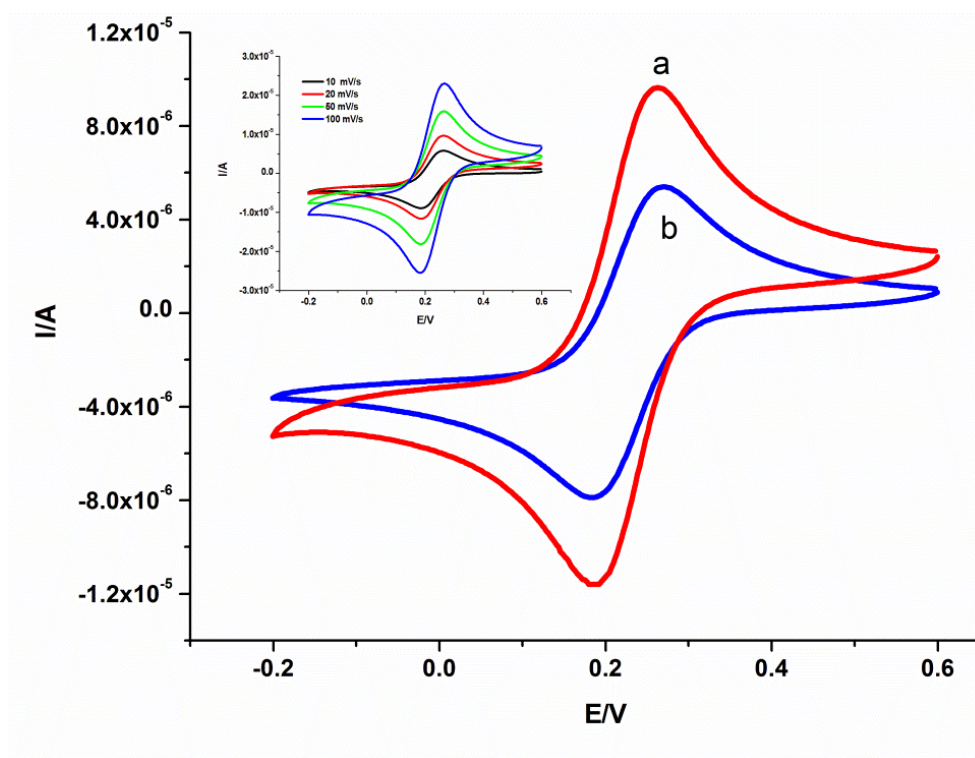


**Figure 3.** Voltammograms of bare GCE (a) and graphene -modified GCE (b) in 4 mM  $\text{K}_3\text{Fe}(\text{CN})_6$ . Supporting electrolyte: 1.0M  $\text{KNO}_3$ ; scan rate: 20 mV/s. Inset : CV overlay at different scan rates for 2 mM  $\text{K}_3\text{Fe}(\text{CN})_6$  at graphene- modified GCE.

The current increase from  $5.52\text{ }\mu\text{A}$  of the bare GCE to  $9.89\text{ }\mu\text{A}$  of the graphene-modified GCE shows that graphene enhances the sensitivity of the glassy carbon electrode. The linear dependence of oxidation and reduction peak currents on the square root of the scan rate showed that the process is diffusion controlled as shown in the inset of Figure 3. A correlation of 0.984 was obtained. The graph presented in the inset can also be used as a measure of the stability of the graphene film.

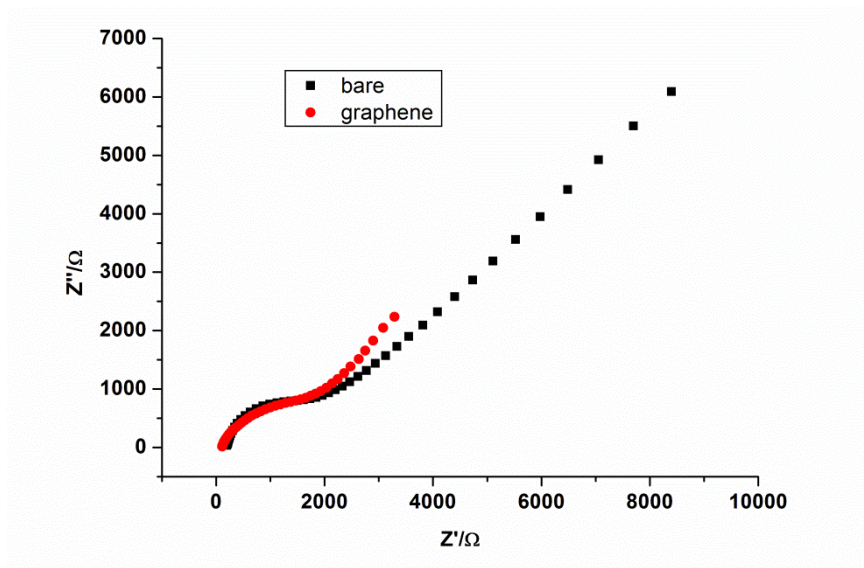


**Figure 4.** EIS of bare and modified- GCEs in 2 mM  $K_3Fe(CN)_6$ .

### 3.3. Electrochemical oxidation of Bisphenol A.

Cyclic voltammograms for oxidation of BPA in 0.1 M phosphate buffer solution at bare and modified GCE are shown in Figure 5. The oxidation peak currents of BPA were found to be 4.45  $\mu A$  (curve b) and 12.8  $\mu A$  (curve c) for bare and graphene-modified GCE respectively. However, there was no peak observed in curve a, suggesting that the peaks found in curve b and c are undoubtedly assigned to BPA. The enhancement of oxidation peak current at graphene-modified GCE reveals that graphene exhibit electro-catalytic behavior towards the electrochemical oxidation of BPA due to its fast electron transfer capability (see figure 3 and Figure 4).

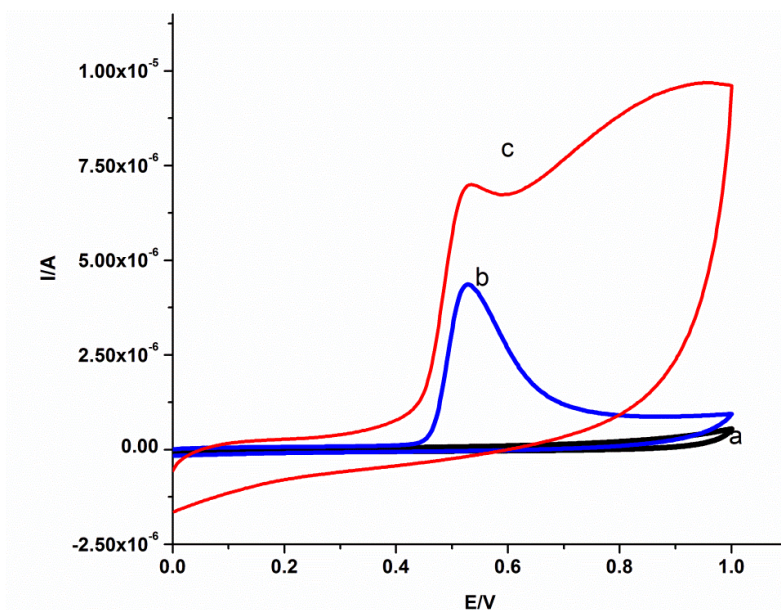


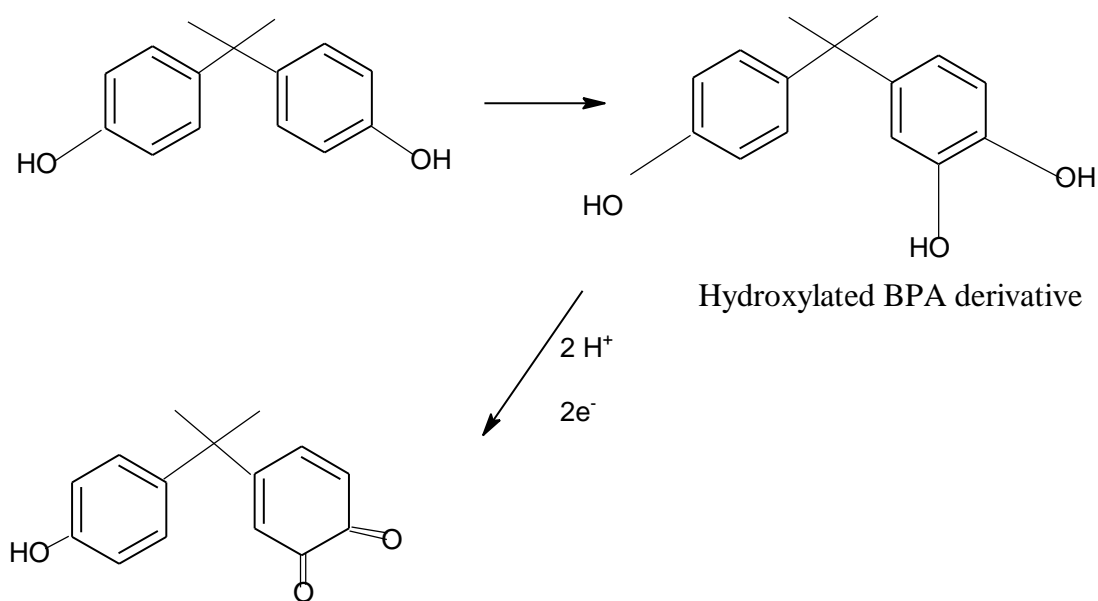
**Figure 5.** Cyclic voltammograms of (a) blank (PBS), (b) 1 mM BPA at bare GCE and (c) 1 mM BPA at graphene-modified GCE. Supporting electrolyte: PBS pH 7. Scan rate: 20mV/s

A pronounced potential shift (indicating kinetic effect) would have been observed if there was leaching or instability in the drop coated film but this was not the case. The charge transfer resistance was studied using electrochemical impedance spectroscopy (Figure 4).

The charge transfer resistances were found to be 1.588 k $\Omega$  and 2.377 k $\Omega$  for graphene modified and bare GCE respectively using the simple Randle's equivalence circuit fitting. The lower charge transfer resistance indicates that graphene exhibits fast electron transfer kinetics due to  $\pi$ - $\pi$  stackings which allows electrons to move without scattering mobilities.

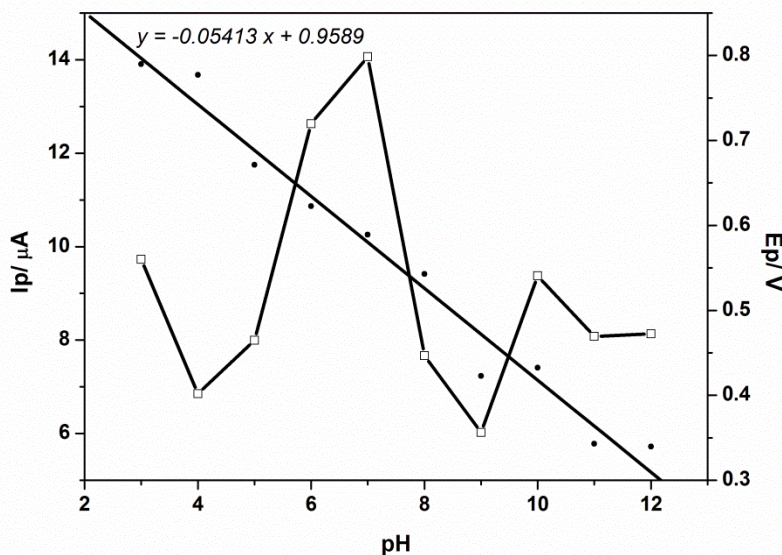
#### 3.4. Optimization of experimental conditions.

**Influence of pH:** The effect of pH on the oxidation peak current and peak potentials of BPA on graphene-modified GCE was investigated with pH ranging from 3 to 12 as shown in Figure 6. The peak current was higher at neutral medium (pH 7). The maximum response to pH was lower than the pKa of Bisphenol A (pKa = 9.73) [15]. This is due to the adsorption of non dissociated BPA on graphene-modified GCE surface [15,16]. The peak shifted towards lower potential with increasing pH value. The same trend was also observed for the bare GCE. This is due to the fact that at lower pH, there is an excess of H<sup>+</sup> from the supporting electrolyte which tends to compete with those of the analyte. Therefore, for oxidation of BPA to occur, a driving force (energy) is required, thus the peak occurs at higher potentials. The slope of E<sub>pa</sub> vs. pH was found to be 54 mV/pH which was close to the theoretical value 57 mV/pH. The closeness of the slopes shows that equal number of electron transfer was accompanied by an equal number of proton in the electrode reaction [1]. Therefore, the electro-oxidation of bisphenol A in the presence of graphene is a two-electron and two-proton process as shown in scheme 1:



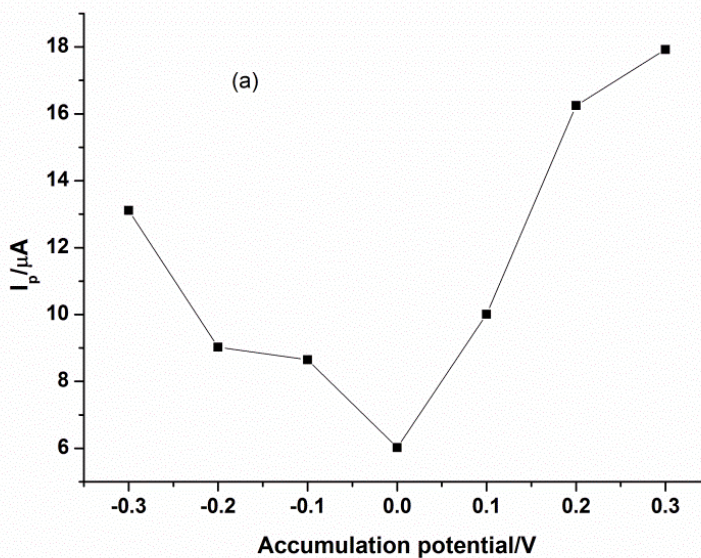
**Scheme 1.** Proposed mechanism for electrochemical oxidation of BPA.





**Figure 6.** Plots peak current (□) and potential (●) of Bisphenol A with variation of pH at graphene-modified GCE.

**Effect of accumulation potential and time:** Differential pulse voltammetry (DPV) is an effective and common used electroanalytical technique when the content of analyte is very low since it possesses high sensitivity. Investigation of the influence of accumulation time and potential as well as the current response on various concentrations was carried out using DPV. The influence of accumulation potential on the oxidation peak current of BPA at graphene-modified GCE is shown in Figure 7 using 5s as a pre-concentration time.



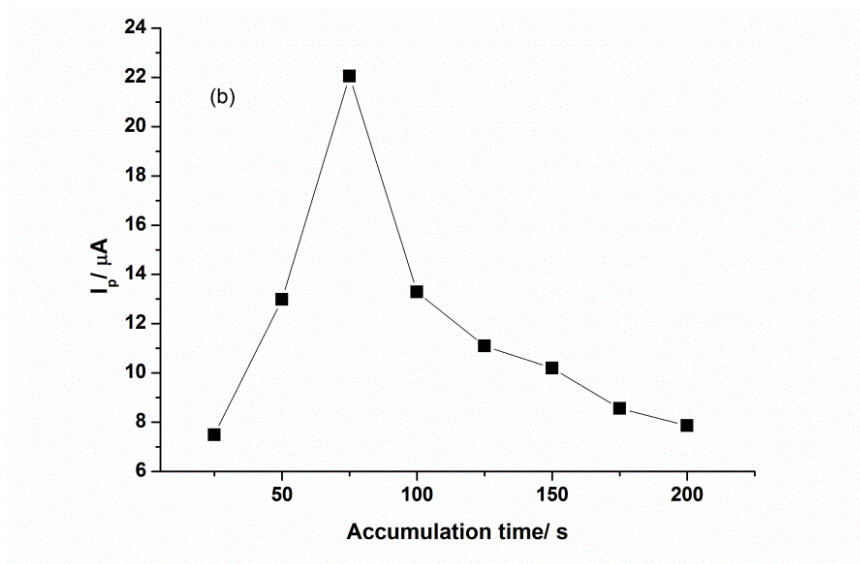


**Figure 7.** Effect of (a) accumulation potential and (b) time in  $1 \times 10^{-6}$  mol/L BPA, 0.3V.

The oxidation peak current was found to be higher at more positive potential (0.3V). In addition, the peak current increased with time but after 75 s, the peak current diminished which indicates that a limiting value of the amount of BPA on the electrode surface had been reached. Thus optimum conditions are: 0.3V (accumulation potential), 75 sec (accumulation time) and PBS at pH 7.

3.5. Determination of detection limit

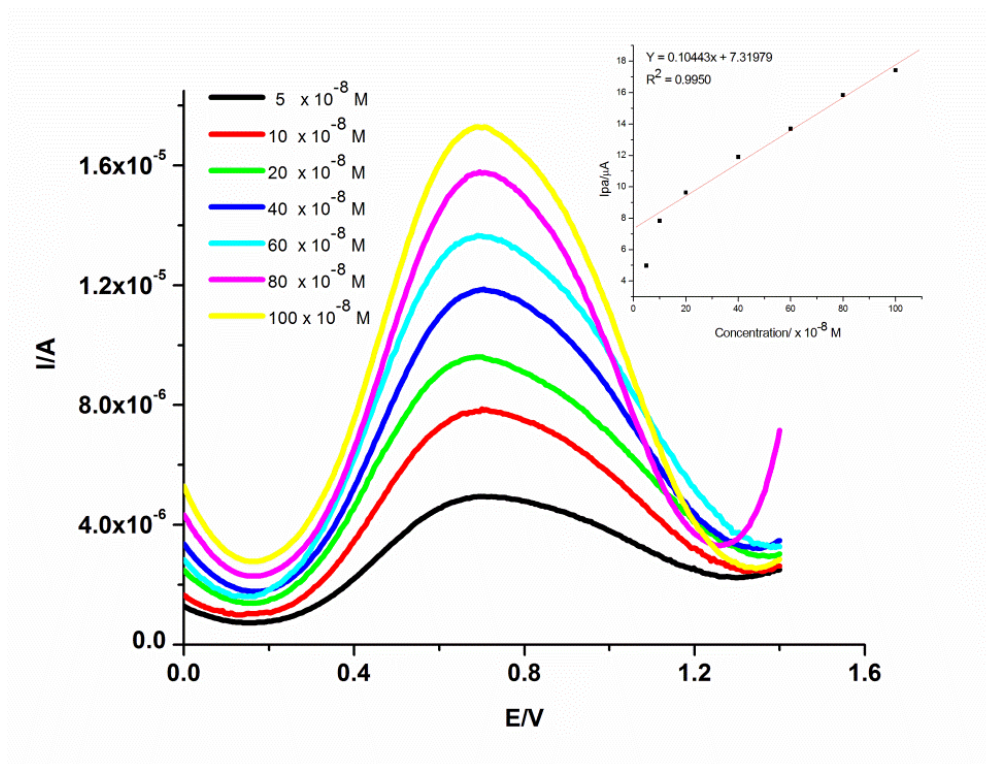


**Figure 8.** Voltammograms of BPA at various concentration.

The electrochemical oxidation of BPA was determined over a concentration range of  $5 \times 10^{-8}$  mol L<sup>-1</sup> to  $1 \times 10^{-6}$  mol L<sup>-1</sup> as shown in Figure 8. The calibration plot shows a linear relationship with a correlation coefficient of 0.9950 ( $n = 7$ ), obeying the equation:

$$i_p = 0.010443 \mu\text{A L mol}^{-1} \times [\text{BPA}] + 7.3197$$

The formula  $3\sigma/\text{slope}$  was employed to calculate detection limit, where  $\sigma$  is the standard deviation of the blank. Under the optimized conditions, the detection limit of this method is  $4.689 \times 10^{-8}$  M. The detection limit was found to be in good agreement with those reported in literature [2, 17,18, ].

### 3.6. Analytical application of graphene-modified GCE

The suitability and potential of graphene-modified GCE for sample analysis was demonstrated by determining BPA in real sample. The BPA was extracted from mineral water plastic bottle purchased from a local supermarket. The detected concentration was  $3.65 \mu\text{M}$  with a recovery of ca. 90 %.

## 4. CONCLUSION

A sensitive and reliable electrochemical method for detection of BPA in real samples using graphene as modifier is proposed. Upon modification with graphene, the oxidation peak current of BPA was significantly improved due to high catalytic activity and conductivity of graphene. Under the optimized conditions, the detection limit was found to be  $4.689 \times 10^{-8}$  M which is comparable to other electrodes and of economic significance. Owing to the high sensitivity of graphene-modified GCE, this method may be used for the detection of other phenolic compounds in food or biological fluids.

## ACKNOWLEDGEMENTS

This work was financially supported by the Nanotechnology Innovation Centre, Mintek and the Faculty of Science, University of Johannesburg, South Africa.

## References

1. H. Yina, Y. Zhou, J. Xu, S. Ai, L. Cui and L. Zhu, *Anal. Chim. Acta*, 659 (2010) 144
2. H.-s. Yin, H. Y.-l. Zhou and S.-y. Ai, *J. Electroanal. Chem.*, 626 (2009) 80
3. X. Liu, H. Feng, X. Liu and D. K. Y. Wong, *Anal. Chim. Acta*, 689 (2011) 212
4. W. Huang, *Bull. Korean Chem. Soc.* 20 (2005) 1560
5. T. Ndlovu, O. A. Arotiba, R. W. Krause, and B. B. Mamba, *Int. J. Electrochem. Sci.*, 5 (2010) 1179 – 1186.6.

6. K. S. Novoselov, A. K. Geim, S. V. Morozov, D. Jiang, Y. Zhang, S. V. Dubonos, I. V. Grigorieva and A. A. Firsov, *Science*, 306 (2004) 666
7. A. K. Geim and K. S. Novoselov, *Nat. Mater.*, 6 (2007) 183
8. M. Pumera, A. Ambrosi, A. Bonanni, E. L. K. Chng and H. L. Poh, *Trends in Analytical Chemistry*, 29 (2010) 954
9. Y. Shao, J. Wang, H. Wu, J. Liu, I. A. Aksay and Y. Lina, *Electroanalysis*, 22 (2010) 1027.
10. G. Wang, J. Yang, J. Park, X. Gou, B. Wang, H. Liu and J. Yao, *J. Phys. Chem., C* 112 (2008) 8192
11. K. Zhang, Li Li Zhang, X. S. Zhao and Jishan Wu, *Chemistry of Materials* 22 (2010) 1392
12. H. Kuramitz, Y. Nakata, M. Kawasaki and S. Tanaka, *Chemosphere.*, 45 (2001) 37
13. A. Das, B. Chakraborty and A. K. Sood, *Bull. Mater. Sci.*, 31 (2008) 579
14. G. Eda and M. Chhowalla, *Adv. Mater.*, 22 (2010) 2392
15. H. Sambe, K. Hoshina, K. Hosoya and J. Haginaka, *J. Chromatogra.*, A 1134 (2006) 16
16. L. Fernandez, C. Borrás and H. Carrero, *Electrochim. Acta*, 52 (2006) 872
17. Y. Q. Wang, Y. Y. Yang, L. Xu and J. Zhang, *Electrochim. Acta*, 56 (2011) 2105-2109
18. F. R. Wang, J. Q. Yang and K. B. Wu, *Anal. Chim. Acta*, 638 (2009) 23